isothermal heat treatments. Acta Materialia. 2003. Vol. 51. pp. 6077–6094.

8. Xu Fang, Yong Du, Min Song, Kai Li, Chao Jiang. Effects of Cu content on the precipitation process of Al – Zn – Mg alloys. Journal of Materials Science & Technology. 2012. Vol. 47. pp. 8174–8187.

9. Marlaud T., Deschamps A., Bley F., Lefebvre W., Baroux B. Evolution of precipitate microstructures during the retrogression and re-ageing heat treatment of an Al – Zn – Mg – Cu alloy. Acta Materialia. 2010. Vol. 58. pp. 4814–4826. doi: 10.1016/j.actamat.2010.05.017

10. Zolotorevskiy V. S., Belov N. A. *Metallovedenie liteynykh aluminievykh splavov* (Materials Science of Casting Aluminum Alloys). Moscow : MISiS, 2005. 376 p.

11. Zolotorevskiy V. S., Belov N. A. Materials Science of Casting Aluminum Alloys. MISiS : Moscow, 2005. 376 p.

12. Belov N. A., Zolotorevskiy V. S. Liteynye splavy na osnove aluminievo-nikelevoy evtektiki (nikaliny) kak vozmozhnaya alternativa siluminam (Casting alloys based on aluminum–nickel eutectic (nikalins) as a possible alternative for silumins). T*svetnye Metally = Non-ferrous metals*. 2003. No. 2. pp. 99–105.

13. Belov N. A., Zolotorevskiy V. S. The effect of nickel on the structure, mechanical and casting properties of 7075 aluminum alloy. Materials Science Forum. 2002. 396–402.

14. Pat. 2245383 RF. Aluminum-base material/ Belov N. A. et al. *Byull. Izobr. Polezn. Modeli*, 2005. No. 3.

15. Belov N. A., Tagiev E. E. Eutectic structures in alloys based on solid solution of the Al – Zn – Mg – Cu system. Izv. Vysh. Ucheb. Zaved., Tsvetn. Met. 1991. Vol. 2. pp. 95–98.

16. Lijun Zhang, Jiong Wang, Yong Du, Rongxiang Hu, Philip Nash, Xiao-Gang Lu and Chao Jiang. Thermodynamic properties of the Al – Fe – Ni system acquired via a hybrid approach combining calorimetry, first-principles and CALPHAD. Acta Materialia. 2009. Vol. 57. pp. 5324–5341. doi: 10.1016/j.actamat.2009.07.031

17. Mondolfo L. F. *Structura I svoystva aluminievykh splavov* (Structure and Properties of Aluminum Alloys). Moscow : Metallurgiya, 1979. 640 p.

18. Zakharov M. *Promyshlennye splavy tsvetnykh metallov* (Commercial alloys of non-ferrous metals). Moscow : Metallurgiya, 1980. 256 p.

NFM

# Modeling of butt and lap joint laser welding of aluminum alloys and constructional steel sheets

UDK 621.791.725

***A. N. Shlegel***, *Head of Laboratory of the laser technologies research and application of the Engineering Center, Assistant Professor of Automation of technological processes Department* [1], *e-mail: shlegel81@rambler.ru*
***N. N. Evtikheev***, *Head of Laser Physics Department*[2]
***D. S. Gusev***, *Engineer of Laboratory of the laser technologies research and application of the Engineering Center*[1]
***A. B. Ivanchenko***, *Assistant Professor, Mechanical Engineering Department*[1]

[1] *Vladimir State University named after Alexander and Nikolay Stoletovs, Vladimir, Russia.*
[2] *National Research Nuclear University MEPhI (Moscow Engineering Physics Institute), Moscow, Russia.*

Recently the most claimed at the market are technologies of body components and parts obtaining which combine multi-metal welding. Such technologies are especially needed on the railway and motor transport as well as in special production. Manufacturing of the motor transport frame units consisting of steel skeleton and sheet aluminum coating allows to improve their corrosion resistance and essentially decrease weight of the carriers, which consequently contribute to the fuel consumption lowering. Residual deformations originated from the welding process negatively affect the welded construction qualitative characteristics, such as strength, harshness, containment, corrosion resistance, etc. Stress level reduction is available by means of the welded seam form and quality, which depend on the welding process technological parameters. Determination of rational technological parameters of the welding processes requires taking into account the used rolled metal features, namely different thermal conduction of materials, significantly bigger (≈50%) coefficient of linear (thermal) expansion inherent to non-ferrous metals as compared to carbon steel, foamed metal-oxide layer formation on the surface of the weld leading to deterioration of corrosion resistance.
The article is devoted to the modeling process of the laser welding modes impact upon strength properties of the weld of aluminum alloy and constructional steel sheets. Presented are an algorithm and results of the finite-element analysis simulation modeling of the butt and lap joint laser welding by the example of AMg2M (АМг2М) aluminum alloy and St3 (Ст3) steel samples. Weld strength properties obtained experimentally and by modelling are compared. It is demonstrated that the worked out simulation model of multi-metal sheets laser welding may be used for theoretical study of the butt and lap joint welding of any other heterogeneous materials.

**Key words:** laser welding, lap joint welding, butt welding, simulation model, method of finite-element analysis, aluminum alloy, steel, residual stresses, ultimate breaking load, tensile strength.

***DOI:*** *http://dx.doi.org/10.17580/nfm.2016.01.05*

## Introduction

Manufacturing of the motor transport body components consisting of steel skeleton and sheet aluminum coating allows to improve their corrosion resistance and essentially decrease weight of the carriers, which consequently contribute to the fuel consumption lowering.

Elaboration of scientifically sound recommendations on the laser welding rational modes providing purposive forming of desired properties of the welds of aluminum alloy and constructional steel sheets with different thickness, is a topical problem in the motor transport frame units manufacturing.

The article is focused on the theoretical study and experimental research sounding an investigation of the laser welding modes impact upon the weld strength properties.

Weld strength properties are essentially affected by level of residual welding stresses, especially if the material is disposed towards brittle failure caused by low characteristics of plasticity and impact elasticity, three-dimensional stress state, operation in the cold brittleness temperature range. Weld durability is distinctly reduced by such factors as tensile residual stresses after welding, stress concentration inserted by the weld as well as an essential deterioration of strength properties in the heat affected zones owing to structural changes. If material works in elastic region, than total stresses are obtained by summarizing residual stresses and stresses of external loads [1–3].

The present study is aimed to:

1. Development of a simulation model for laser welding of heterogeneous materials sheets with different thickness based on the finite-element analysis. The model should allow calculating temperature fields of the welded parts.

2. Working out a procedure for residual welding stresses determination in a weld-adjucent zone during butt and lap joint laser welding of heterogeneous materials sheets with different thickness.

3. Elaboration of estimation procedure for laser emission processing parameters influence over the weld strength properties (static strength) during butt and lap joint laser welding of heterogeneous materials sheets with different thickness.

## Research procedure

To estimate laser emission processing parameters influence over the weld strength properties during laser welding of aluminum alloy and constructional carbon and low-alloy steel sheets the following algorithm is proposed:

– welding samples thermal state modeling based on CAE-systems;

– welding samples stress state caused by temperature influence modeling based on CAE-systems;

– determination of plastic temperature deformations and residual stresses in the heat affected zones;

– modeling the welding samples stress state when mechanically tested on tearing machine rupture-test machine;

– determination of tensile strength in the heat affected zones of samples obtained by mechanical tests on tearing machine rupture-test machine taking into account residual stresses and structural changes ($\sigma_{r_{haa}}/\sigma_r$ rates) for heat affected zones [1].

Simulation modeling has been implemented on specimens of AMg2M aluminum alloy and St3 steel. Such a choice accounts for the fact that these materials are prevalent and the most commonly used for the components of carrier body manufacturing. Lap joint and butt welding were considered.

Thermophysical and mechanical properties of materials of the samples employed in the model were assigned according to reference data: with dependence on temperature (Tables 1, 2) and without it (Table 3) [4, 5]:

Characteristic property of the developed computational model lays in the fact that the weld is forming of fragments consequently providing heat enclosure along

Table 1

**Thermophysical and mechanical properties of the St3 steel depending on temperature**

| Temperature, °C | 20 | 100 | 200 | 300 | 400 | 500 | 600 | 700 |
|---|---|---|---|---|---|---|---|---|
| Thermal conduction coefficient λ, *W*/(*m*·*K*) | 55 | 55 | 54 | 50 | 45 | 39 | 34 | 30 |
| Elastic modulus *E*, MPa | 213,000 | 208,000 | 202,000 | 195,000 | 187,000 | 176,000 | 167,000 | 153,000 |
| Yield point $\sigma_{0.2}$, MPa | 274 | 243 | 230 | 185 | 166 | 150 | 120 | – |

Table 2

**Thermophysical and mechanical properties of AMg2M aluminum alloy depending on temperature**

| Temperature, °C | 20 | 100 | 200 | 300 | 400 |
|---|---|---|---|---|---|
| Thermal conduction coefficient λ, *W*/(*m*·*K*) | 155 | 159 | 163 | 163 | 168 |
| Elastic modulus *E*, MPa | 71,000 | 69,000 | 63,000 | 51,000 | 33,000 |
| Linear expansion coefficient $\alpha_T$, 1/K | 0.000024 | 0.000024 | 0.0000268 | 0.0000288 | 0.0000294 |
| Yield point $\sigma_{0.2}$, MPa | 100 | 95 | 70 | 35 | – |

Table 3

**Thermophysical and mechanical properties of St3 steel and AMg2M aluminum alloy**

| | St3 | AMg2-M |
|---|---|---|
| Density ρ, kg/m$^3$ | 7850 | 2680 |
| Specific heat $c$, J/(kg·K) | 500 | 963 |
| Linear expansion coefficient $\alpha_T$, 1/K | 0.000014 | – |
| Poisson's ratio, $Y$ | 0.32 | 0.33 |
| Tensile strengtht $\sigma_r$, MPa | 430 | 210 |

Table 4

**Experimentally obtained weld pool parameters**

| Parameters | Joint | |
|---|---|---|
| | butt | lap joint |
| Weld pool length, mm | 0.5 | 0.75 |
| Weld pool depth, mm | 3 | 3.3 |
| Weld pool width, mm | 1 | 0.70–0.78 |
| Width of heat affected zone for AMg2M alloy, mm | 0.2 | 0.04 |
| Width of heat affected zone for St3 steel, mm | 1 | 0.75 |
| Time of beam traverse above the weld pool, s | 0.01 | 0.025 |

the length of it, while their geometric dimensions mould a volume, corresponding to the weldpool size. In the course of solving a problem, fragment temperature is changing along the second-order curve from the temperature exceeding melting-point of the more refractory metal to the melting temperature of the less refractory one. This change is taken place during time slice depending on the laser beam traverse speed and its length.

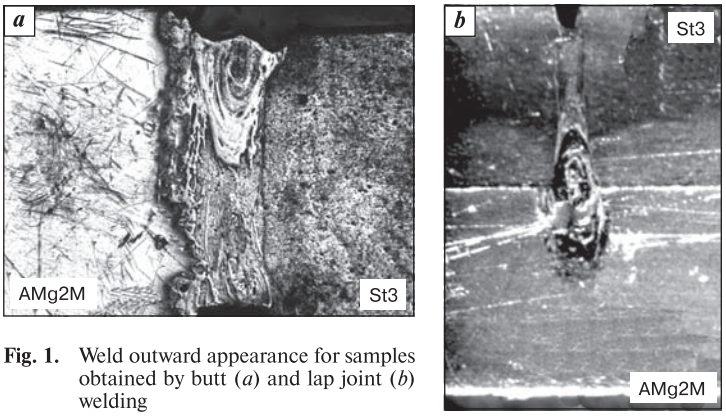


**Fig. 1.** Weld outward appearance for samples obtained by butt (*a*) and lap joint (*b*) welding

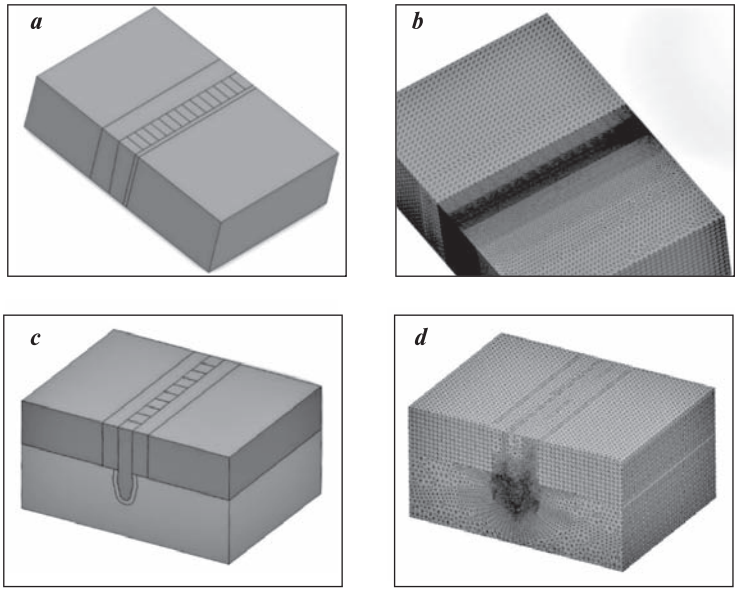


**Fig. 2.** Solid-state (*a*) and finite-element (*b*) models of the butt welded sample and solid-state (*c*) and finite-element (*d*) models of the lap joint welded sample

It is obvious, that accuracy of calculation results mainly depends on correctness of the weld pool parameters and its temperature spread determination [6–8]. For geometrical dimensioning of partition grid parameters which make welded seam as well as the width of heat affected zonesheat affected zones, real dimensions of the samples weld obtained by butt and lap joint welding were used (Fig. 1).

As a result of study of five specimens for each weld type, there were determined average values of the fragments corresponding to the weld pool as well as the width of a heat affected zone. Thus, the weld pool parameters obtained for welding conditions as $P = 3000$ W and beam traverse speed as $v = 50$ mm/s for butt welding and welding conditions as $P = 1600$ W and beam traverse speed as $v = 30$ mm/s for lap joint welding are presented in the Table 4. Heat affected zone value on the side of aluminum was visually determined by means of inverted microscope Nikon Epiphot TME 200. This side possesses more dark microstructure and insignificant microhardness increase in area close to welded connection point as compared with source aluminum material at cross microsections of the weld.

First step of the finite-element modeling is a three-dimensional model developing for subject of inquiry. Then they determine finite elements type and size, specify physical and mechanical properties of material depending on temperature, assign boundary conditions. Solid-state simulation software SolidWorks were used for 3D-model making. Modeling of heat processes existing during welding was fulfilled in environment of CAE complex SolidWorks Simulation. Four-component finite element was used to fix a thermal state of a part. Finite-element model consisted of 643,190 nodes and 3,781,417 elements for a butt joint and of 211,372 nodes and 1,239,183 elements for a lap joint with transverse weld. Average rib size of finite element in the heat affected zones made up 0.03–0.05 mm, for the rest of the model it was equal to 0.2 mm.

In the process of modeling there were considered half of the specimen cutting off by longitudinal symmetry plane. This allowed guaranteeing the rational combination of required computational resources without degradation of accuracy. Both solid-state and finite-element models are represented in Fig. 2.

Welding of samples was carried out in one pass. Time domains for design regimes came to: 0.3 s for butt welding and 0.5 s for lap joint welding. This time domains were divided into slots according to the time of beam traverse upon the weld part equal to the weld pool length, i. e. 0.01 s and 0.025 s. For corresponding weld fragment within each time domain there were settled the I type boundary conditions in accordance with the weld pool temperature changes curve (1400–600 °C), time slot for each domain was 0.0005 s. Temperature field obtained at the last step served as a starting condition for a following time domain. Cooling down of the samples surfaces in process of welding fitted with conditions of free convection, that is at the corresponding surfaces there were settled the III type boundary conditions: heat transfer coefficient as 50 W/m$^2$·K and ambient temperature as 27 °C.

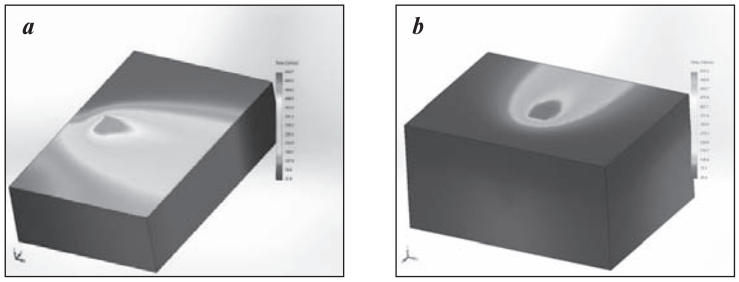


**Fig. 3.** Sample temperature distribution in the weld zone during butt welding for 0.09 s (*a*) and during lap joint welding for 0.1 s

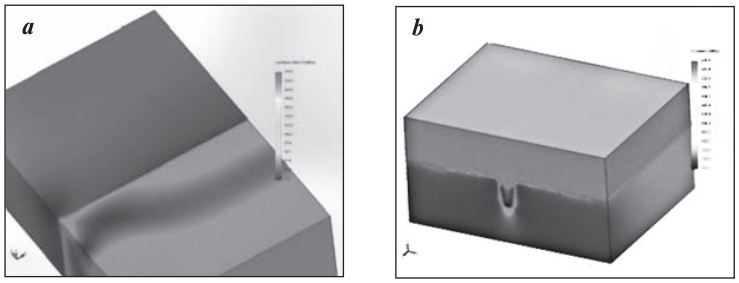


**Fig. 4.** Equivalent stress fields (von Mises) of the butt welded samples (*a*) at the cooling down stage (0.05 s); stress fields $\sigma_3$ of the lap joint welding samples (*b*) at the cooling down stage (0.5 s)

## Results

Temperature fields of the lap joint and butt welded samples are represented in Fig. 3.

Calculation of stress state of the samples was carried out for the first second of cooling, since the beginning of cooling indeed is connecting with plastic compressive strains, which cause residual stresses. Target setting have corresponds with the finite-element realization of the thermoelasticity theory.

Stress state of the welded samples at cooling stage (0.05 s) is represented in Fig. 4.

Analysis of the temperature and stresses distribution at the AMg2M alloy heat affected zone (Fig. 5) shows that along the full length of the welded seam stresses level exceeds the yield point of the material. That is plastic deformations develop and cause residual stresses after the sample cooling down.

During the butt welding, stress state is close to the single-axis one. At the same time, during the lap joint welding we obtain a three-dimensional compound stress due to the welded seam implantation into the section of an AMg2M alloy sample.

It is known that the peak level of residual welded stresses is typical of the fusion zone at the point of a change-over from welded seam to base metal, and such a zone indeed determines static strength of welded components. Thus, calculations of plastic deformations in this zone were based on dependences obtained by use

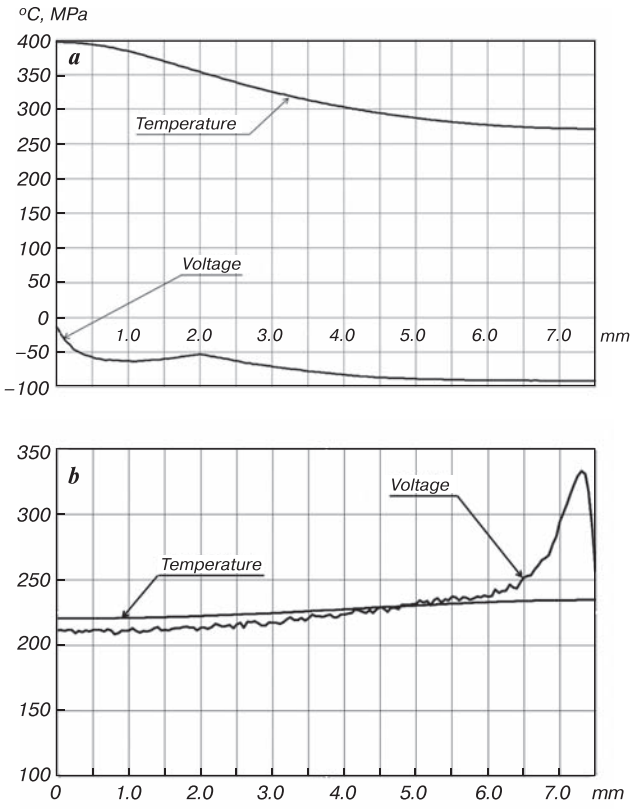


**Fig. 5.** Temperature and stresses $\sigma_3$ distribution in the AMg2M alloy heat affected zone in case of butt welding for a 0.05-s cooling down (*a*); temperature and von Mises equivalent stresses distribution in the AMg2M alloy heat affected zone in case of lap joint welding for a 0.05-s cooling down (*b*)

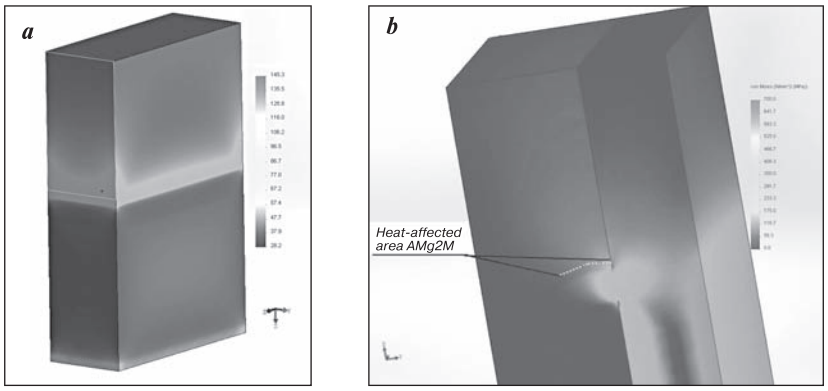


**Fig. 6.** Von Mises equivalent stress field for the butt welded samples under the load of 180 kgf (*a*) and for the lap joint welded samples under the load of 160 kgf (*b*)

of the Neiber generalized principle and deformation criteria of limiting state [9, 10]:

$$\sigma_f = 1.75\sigma_r; \quad (1)$$

$$\varepsilon_f = 0.76[\ln(1/(1-\psi))]^{0.6}, \quad (2)$$

here $\sigma_r$, $\psi$ — tensile strength and relative narrowing of material on rupture; $E$ — elastic modulus; $\sigma_{lin}$ — stress obtained as a result of the thermoelasticity task solution; $b = -0.9...-0.12$ — for deformable materials; $c = -0.5...-0.6$ — for deformable materials; $m = 0.1$ — for temperature loading [11].

Using the flow theory realized in the context of the finite-element analysis [2, 3] is complicated by the fact that the samples' temperature field varies in a wide range during the welding process. On application of the flow theory, it is not feasible to correctly describe deformation curves for temperatures close to melting temperature of materials. But for solving the suggested equations it is enough to carry out a thermoelastic calculation and to apply reference data on mechanical characteristics of material.

Calculation of plastic deformations forming in the weld-adjacent has been carried out for high-beat state of samples, corresponding to 0.05 s in case of butt welding and 0.5 s in case of lap joint welding at cooling stage. Zone on AMg2M side has been observed, because its strength properties are substantially lower then those of St3 steel. Temperature in the designed area has been changed along the weld seam between 230 and 359 °C for butting and between 240 and 270 °C for splice. Linear temperature stresses $\sigma_{3lin} = 90–50$ MPa for butting and $\sigma_{eq.lin} = 220–250$ MPa for splice. According to the temperature range for AMg2M, $\sigma_r = 140–30$ MPa, $\psi = 0.9–0.6$. In case of butt welding, stress state is close to the single-axis one. That's why absolute peak compression stresses were considered, that is $\sigma_{3lin}$. During the lap joint welding we obtain a three-dimensional compound stress due to the welded seam implantation into the section of an AMg2M alloy sample. Therefore, residual stresses were determined by use of equivalent stresses calculated by the Huber – Mises – Hencky hypothesis, that is $\sigma_{eq.lin}$. Absolute values of designed temperature plastic deformations in the weld-adjacent zone have amounted $\varepsilon_{pl} = 0.0012–0.0013$ for butting and $\varepsilon_{pl} = 0.0021–0.0025$ for splice. Level of residual stresses made up $\sigma_{rez} = 86–96$ MPa and $\sigma_{rez} = 140–160$ MPa respectively.

Tensile strength for the heat affected zone of AMg2M alloy have been determined according to the results of conditions modeling for butt and lap joint welded samples loading on a tensile test machine. Load have been changed proportionally from 0 to 300 kgf in a 5-s loading time. Calculation results are represented in the Fig. 6.

The peculiarity of a finite-element model for calculating the lap joint welded samples stress of a breaking load lied in the contact elements, included into the model to ensure possibility of the movements of the samples relative to each other.

Changes of strength properties of material in the heat affected zone have been took into consideration while estimating the tensile strength of the butt welded sample. For deformable alloys AMg2 (АМг2), AMg3 (АМг3), AMg5 (АМг5), AMg6 (АМг6), the weld-adjacent zone damping factor is within the limits of 0.8–0.9 [12]. Stress diagrams for the weld-adjacent zone at the loading stages were obtained as a result of composing tensile load stresses of a rupture machine and residual welding stresses (Fig. 7).

Implemented strength analysis of a butt sample for residual stresses level of 86–96 MPa and AMg2M tensile strength of 180 MPa made it clear, that the failure load is within the limits of 200–240 kgf, which corresponds to the weld's tensile strength or $\sigma_r = 84–94$ MPa.

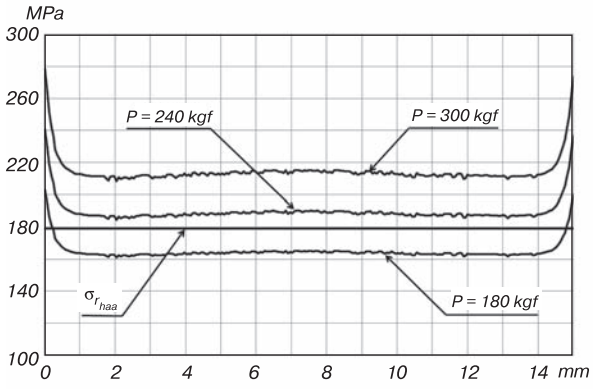


**Fig. 7.** Tensile strength and stress diagrams at loading stages for the AMg2M alloy heat affected zone in case of butt welding

Range of stress changes for the alloy heat affected zone in case of lap joint welding is as follows:

- for load $P$ = 160 kgf it is 50–60 MPa;
- for load $P$ = 240 kgf it is 80–90 MPa.

In view of the residual stresses level of 140–160 MPa and AMg2M tensile strength of 210 MPa and without taking into consideration the weld-adjacent zone damping factor, since the base material is also in the ruptured zone, failure of the sample should have place at the load of 160–170 kgf, which conforms to the weld's tensile strength of 50–70 MPa.

As a result of experimental study on the rupture machine of five-samples lots of similar welded pairs with suitable engineering parameters, average values of ultimate load come to the following:

– for butting it is 215 kgf;

– for splice it is 168 kgf.

Difference between the modeling and experimental results amounts to 1.8–2.3%.

## Conclusion

*1. Simulation in the context of the designed procedure of determination of residual welding stresses in the weld-adjacent zone in case of laser welding have showed that the weld's residual stress level, given the laser welding of heterogeneous materials by example of AMg2M and St3, is considerable (for butting it is 86–96 MPa; for splice it is 140–160 MPa). This leads to deterioration of the weld's strength parameters.*

*2. Mode of samples' failure is testimony to high brittleness in the AMg2M fusion zone, which is concerned with aluminum temperature overheating and formation of fragile intermetallide phases like* $FeAl_2$, $Al_5Fe_2$, $AlFe_3$.

*3. Elaborated estimation procedure of the laser welding processing parameters influence over the welding seam strength properties allowed to determine, how deterioration of the welding seam strength properties in comparison with base material depends on operating modes. Lessening exceeds 40% for butt welding and 60% for lap joint welding, which is related to the weldpool volume expansion and intermetallic compounds formation rate.*

*4. The worked out simulation model of the sheets of heterogeneous materials laser welding allowed to correctly calculate breaking load for selected types of connection and parameters of engineering process. Relative deviations of the theoretical research results from those obtained at the tensile test machine come to the following: for butting — 2.3%; for splices — 1.8%, which verifies the worked out simulation model adequacy.*

5. *The worked out simulation model of multi-metal sheets laser welding may be used for modeling the butt and lap joint welding of any other dissimilar materials.*

***The work was supported by the Ministry of Education and Science of the Russian Federation.***

***Agreement on grant No. 14.577.21.0158 of November 28, 2014. Unique identifier PNIER (ПНИЭР) RFMEFI57714X0158.***

## References

1. Birger A. I. *Ostatochnye napryazheniya* (Residual stresses). Moscow : Mashgiz, 1963. 232 p.

2. Costa J. M. et al. Residual stresses analysis of ND-YAG laser welded joints Engineering Failure Analysis. 2010. Vol. 17. pp. 28–37.

3. Dai H. Modelling Residual Stress and Phase Transformations in Steel Welds. Neutron Diffraction. 2012. pp. 49–76.

4. Alieva S. G. et al. *Promyshlennye aluminievye splavy: spravochnik* (Commercial aluminum alloys : reference book). Ed. by F. I. Kvasova, I. N. Fridlyander. — 2nd ed., revised and complemented. Moscow : Metallurgiya (Metallurgy), 1984. 527 p.

5. *Marochnik stalei i splavov : spravochnoe izdanie* (Reference book of alloys and steels grades). Ed. by A. S. Zubchenko. — 2nd ed., revised and complemented. Moscow : Mashynostroenie (Mechanical engineering), 2003. 784 p.

6. Shapeev V. P, Isaev V. I., Tcherepanov A. N. Tchislennoye modelirovanye lazernoi svarki stalnykh plastin (Laser welding of steel plates computational modeling). *Fisicheskaya mezomekhanika = Physical mesomechanics.* 2011. Vol. 14, No. 2. pp. 107–114.

7. Sudnik W., Radaj D., Breidschwerdt S., Erofeew W. Numerical Simulation of weld pool geometry in laser beam welding. J. Phys. D: Appl. Phys. 2000. Vol. 33. pp. 662–671.

8. Swapnil R. D., Sachin P. A., Awanikumar P. Finite Element Analysis of Residual Stresses on Ferritic Stainless Steel using Shield Metal Arc Welding. International Journal of Engineering Research and General Science. 2015. Vol. 3. No. 2. pp. 1131–1137.

9. Pospishil B. et al. *Prochnost i dolgovechnost elementov energeticheskogo oborudovaniya* (Durability and longevity of power equipment pieces). Ed by V. N. Kiselevskiy. Kiev : Naukova Dumka, 1987. 216 p.

10. Pospisil B. Zobecneni Neuberova principu smerodatne deformace k vypoctum v oblasti stridave plastike deformace. Strojirenstvi. 1975. Vol. 25. No. 2. S. 74–78.

11. Troshchenko V. T. Rasseyannoye ustalostnoye povregdeniye metallov i splavov. Soobshcheniye 3. Deformatsionnye i energeticheskiye kriterii (Diffused fatigue damage of metals and alloys. Report 3. Deformation and energetic criteria). *Problemy prochnosty = Problems of Durability.* 2006. No. 1. pp. 5–31.

12. Shiganov I. N., Shakhov S. V., Kholopov A. A. *Lasernaya svarka aluminievykh splavov aviatsionnogo naznacheniya* (Laser welding of aviation aluminum alloys). Vestnik MGTU im. N. E. Baumana. Ser. "Mashynostroenie" (Herald of the Bauman Moscow State Technical University. Series Mechanical Engineering). 2012. No. 6. pp. 34–50.